

An Earth-Like Planet in GJ 832 System

S. Satyal^{1*}, J. Griffith¹, Z. E. Musielak^{1,2}

¹*The Department of Physics, University of Texas at Arlington, Arlington TX 76019*

²*Kiepenheuer-Institut für Sonnenphysik, Schöneckstr. 6, 79104 Freiburg, Germany*

ABSTRACT

Stability of planetary orbits around GJ 832 star system, which contains inner (GJ 832c) and outer (GJ 832b) planets, is investigated numerically and the detailed phase-space analysis are performed. The stability of the system is defined in terms of its *lifetime*, which is its survival time during the orbital integration period, and the maximum eccentricity, e_{max} attained by the orbits during the evolution processes. A special emphasis is given to the existence of stable orbits for an Earth-like planet that is injected between the inner and outer planets. Thus, numerical simulations are performed for three and four bodies in elliptical orbits (or circular for special cases), and a large number of initial conditions that covers the whole phase-space of the existing bodies are used. The results presented in the phase-space maps for GJ 832c indicates the least deviation of the eccentricity from its nominal value, which is then used to determine its inclination regime. Also, the Earth-like planet displays stable orbital configurations for at least one billion years. Then, the radial velocity curves based on the signature from the Keplerian motion are generated for the Earth-like planet to estimate its distance from the star and its mass-limit. The synthetic RV signal suggests that an additional planet ($1M_{\oplus} \leq \text{mass} \leq 15M_{\oplus}$) with dynamically stable configuration may be residing between 0.25 - 2.0 AU from the star. We have provided an estimated number of RV observations for the additional planet for further observational verification.

Subject headings: Method: Numerical – Planetary systems – GJ 832

1. Introduction

Recent discovery of exoplanets has shown that the multi-planetary systems in compact orbits seem common in the Milky Way Galaxy. For example, Kepler 186 (Quintana 2014) is a five-planet system with the farthest one, Kepler 186f, located at 0.3926 AU and within the habitable zone of the host star. The nearest one, Kepler 186b, is at 0.0378 AU and orbits the star every 3.88 days. Another such planetary system is Gliese 581 (Mayor 2009), which is known to host three planets along with the two others that are not yet confirmed. The three known planets, Gliese 581b, c, e, orbit the star within 0.02815 AU. Not only Earth-size planets but also the existence of super-Earths in compact multiple systems are found to be more

common (Howard 2012; Batalha 2013). With an addition of the third planet in the Kepler 47 system (Orosz et al. 2015), it became the first multi-planet circumbinary system and opened a new chapter for us to understand the planet formation processes and the dynamical compactness of the planetary orbits.

GJ 832 planetary system is another potentially multi-planet system which is currently known to host two planets within 3.6 AU from the M dwarf star, and is located at a relatively close distance of 16.1 light years from the Earth. GJ 832c (inner planet) (Wittenmyer 2014) orbits its star at a distance 0.16 AU away and is potentially a rocky planet with a mass $\geq 5.4 M_{\oplus}$. This planet is located in the inner boundary of the habitable zone, but it is not expected to be habitable mostly due to its close proximity to the star and possibility of

*corresponding author: ssatyal@uta.edu

having dense atmosphere. Orbiting the same star, a distant planet GJ 832b (outer planet), was discovered by Bailey (2009); which is a long-period (~ 3657 days) giant planet at 3.53 AU, with a mass of $0.64 M_J$. Its orbit is well outside the habitable zone, and given its relative position and its mass, it can be assumed that it plays a role of the Jupiter in the Solar System of setting gravitational equilibrium in the system. The main goal of this article is to explore the gravitational effect of the outer planet on the orbital stability of the inner planet as well as on the Earth-like planet injected between the two known planets. In addition, the long-term stability and orbital configurations of the inner and Earth-like planets, with concentration on the evolution of their eccentricity and inclination, is studied in the $a_{pl} - e_{pl}$ and $a_{pl} - i_{pl}$ phase-spaces.

GJ 832 is a main sequence dwarf star of a spectral type M1.5V (Jenkins 2006), mass of $0.45 M_\odot$ (Bonfils 2013), temperature of 3472 K (Casagrande 2008). The size of its conservative habitable zone can be calculated by using the formula provided by Kopparapu (2013). Then, the orbital stability of an Earth-like planet is investigated within the boundaries of this habitable zone.

The best fit orbital parameters of GJ 832 system as obtained from the original discovery papers are given in Table 1 and for the cases when the parameters are unknown, they are either set to zero or set to a range with a fixed step-size. Both of the known planets in GJ 832 system were detected by the Radial Velocity (RV) technique from which the orbital parameters were extracted by using the best-fit solutions. We used these parameters as the initial conditions for starting our numerical simulations. We also used the integrated data from the time evolution of orbital parameters to generate the synthetic RV curves of the known and the Earth-like planets in the system. Moreover, based on the maximum amplitude of the RV curve obtained from the observation of the inner planet, the approximate mass and distance from the star for the Earth-like planet were computed using the RV signature of the Keplerian motion.

This paper is outlined as follows: In Section 2, we describe our numerical simulations; the results are presented and discussed in Section 3; and the paper is concluded with a brief summary of our main results in Section 4.

2. Numerical Simulations

We have considered the motion of the planets of masses, m_{pl} around the central star in the general elliptical as well as the circular cases. To calculate the initial conditions (ICs) in position and velocity and start the integration processes, we used the best-fit orbital elements: semi major axis (a), eccentricity (e), inclination (i), argument of periastris (ω), ascending node (Ω) and mean anomaly (M), which were obtained from the radial velocity measurements (Wittenmyer 2014). The initial inclination of the inner and the Earth-like planets are taken relative to the orbital plane of the star and the outer planet. Thus, any inclination we refer during our investigation is relative to the star - outer planet plane. The stability of the system is defined in terms of its *lifetime*, which is the planet's survival time during the orbital integration period, and the maximum eccentricity, e_{max} displayed as the orbital phase-space maps showing e_{max} attained in the orbital evolution processes.

Using the orbital integration package MERCURY (Chambers 1997, 1999), the built-in Hybrid algorithm was used to integrate the orbits of the system in astro-centric coordinates. MERCURY was effective in monitoring the ejection or collision of the inner and the injected planets due to a close encounter with the star or the outer planet. While integrating the orbits, a time step of $\epsilon = 10^{-3}$ year/step was considered to obtain high precision data and minimize the error accumulation. The change in total energy and total angular momentum was calculated at each time step which fell within the range of 10^{-16} to 10^{-13} during the total integration period of 10 Myr. The data sampling (DSP) was done per day and per year for shorter integration periods and 500 kyr for a billion years integration period. The *lifetime* maps and the maximum eccentricity (e_{max}) maps are generated for multiple (up to 14,400) initial conditions in a_{pl} , e_{pl} and i_{pl} phase-spaces, and they are simulated for 10 Myr. The billion years simulations are performed only for selected single initial conditions.

3. Results and Discussion

3.1. Dynamics of GJ 832c

The orbital parameters (Table 1) of GJ 832c, the inner planet, is not well constrained for its inclination. To investigate the inclination, its orbits are integrated with 14,400 and 8,000 initial conditions (ICs) in varying i_{pl} , a_{pl} , and e_{pl} phase-spaces. We have only considered prograde orbits for i_{pl} that ranges from 0° to 90° , with a step size of 0.5° , a_{pl} ranges from 0.1 AU to 4.0 AU starting from the central star with the step size of 0.05 AU, and e_{pl} that ranges from 0.0 to 1.0 with a step size of 0.05 step. Then, within a block of $[(i_{pl} \text{ or } e_{pl}), a_{pl}]$, each of the ICs mentioned above are set to evolve for 10 Myr. And during this integration period the close encounters, ejections and collisions between the planets and the host star are allowed to occur which marks the stoppage of the integration processes for those ICs. If the integrated orbit survives the total simulation time, then we consider it to be a stable orbit. However, in cases when the integrated bodies eject or collide during close encounters, hence resulting in the instability of the system, we note the time of such event and use that time to create a global dynamical *lifetime* map which displays dynamically stable or unstable regions.

To explore the dynamics of the inner planet, its *lifetime* map (Fig. 1) is created for multi ICs in i_{pl} and a_{pl} phase-space. Each colored pixels in the figure represent the evolution of one IC. The dark blue color in the map indicates the survival of the planet for total simulation time, and the other colors represent instability, indicating that the planet was ejected from the system or collided with the star or the outer planet in less than 10 Myr. The color codes are in the z-axis with index given in the right-hand color-bar. The vertical dashed lines in the figure, labeled as GJ 832c and GJ 832b, represent the best-fit semimajor axis of the planets. At the best-fit location, GJ 832c remains in stable orbits for total simulation period with an orbital inclination as high as 75° . With longer simulation time (> 10 Myr), this inclination regime may significantly be reduced. Another way to look at this stability regime is by monitoring the maximum eccentricity reached by the planet during the integration period, which we discuss in the following paragraphs. Beyond 75° inclination, the planet

collided with the star or ejected from the system due to the increment in e_{pl} values which results in decreased periastron passage around the star. When the perturber, GJ 832b in this case, has eccentric orbits, then due to the Kozai effects (Kozai 1962) the inner orbit's e_{pl} and i_{pl} can reach extremely large values (Satyal 2014; Naoz 2013b; Ford 2000), eventually leading the system towards the instability. The vertical columns observed at 2.25 AU and 2.7 AU are in 2:1 and 3:2 orbital resonances with the outer planet, GJ 832b respectively.

The maximum eccentricity, e_{max} , map (Fig. 2) for the same phase-space, i_{pl} - a_{pl} , shows the decreased stability regions along the i_{pl} regime compared to the previous *lifetime* map. The color coded z-axis in the map represents the maximum orbital eccentricity experienced by the planet during the total integration period. This e_{max} map was obtained by integrating 14,400 ICs for 10 Myr and recording the maximum eccentricity for each state during their time evolution. Therefore, the e_{max} value for each of the states may or may not be equal to the final e_{pl} , but any of these values are expected to rise with significantly increased simulation time.

The e_{pl} evolution is distinct and in increasing order when moving along blue-green-orange-pink regions in the vertical dashed line at 0.16 AU. The blue-green region is where the planet's e_{max} stays less than 0.5. It suggests that the likely i_{pl} value is less than 45° . It is unlikely for the planet to have i_{pl} greater than 45° and still maintain a stable orbit, because the observed trend in the map shows that the e_{max} quickly increases to 0.8 and 0.9 with increasing i_{pl} , and e_{max} value is only expected to rise for longer simulation time. Hence, the blue-green region is the dynamically stable zone for the inner planet where the gravitational perturbation from the outer planet is minimum. The inner planet could be placed anywhere in this zone, and its orbital configuration would remain unaffected by the outer planet. This is assuming that no other bodies are present other than the two observed planets. The dynamics of the region around the inner planet changes with an additional bodies, which we explore in Sec. 3.2.

The unstable resonances due to the outer planet appear more prominent compared with the *lifetime* map. This is because the z-axis represents

the e_{max} that is attained throughout the integration period. And the observed variations in the phase-space suggest that the forced eccentricity is more sensitive to the orbital stability. The resonances observed at 1.40 AU, 1.70 AU, 2.00 AU, 2.25 AU and 2.70 AU are due to the 4:1, 3:1, 7:3, 2:1 and 3:2 orbital resonances with the outer planet, respectively.

The inner planet’s orbital evolution in e_{pl} and a_{pl} phase-space (Fig. 3) also reveals similar resonances with the outer planet and compliments the e_{max} map in different phase-space shown in Fig. 2. The orbital parameters of the planet deviates least from its best-fit values. The e_{pl} in particular remains unchanged with an a_{pl} increasing outward up to 2.2 AU from the location of the star. The best-fit e_{pl} value is along the best-fit a_{pl} values for the both planets and are denoted by the red asterisks. The upper limit in the uncertainty of the best-fit e_{pl} value, 0.31 also deviates least during the full integration period, suggesting that the uncertainty in the e_{pl} can’t be constrained any further from this analysis.

3.2. Dynamics of an Earth-like planet

The known planetary configuration in this system shows a super Earth orbiting at the close proximity, 0.163 AU from the host star, while a gas giant orbits distantly at 3.56 AU (for reference: Mercury orbits the Sun at 0.39 AU and Jupiter at 5.2 AU). Therefore, existence of other Earth-mass planets (could be bigger or smaller than the Earth) between the inner and the outer planets is a plausible scenario. As observed in Figs. 1 and 2, a body with the mass $5.4 M_{\oplus}$ maintains stable orbits with low enough eccentricity in the regions extending from 0.1 AU to 2.25 AU, with some exception of the resonances which limit the stability region. Excluding those resonance structures, the dark blue-green region remains the orbitally stable zone. To observe how this region evolves with an additional bodies, we injected a third planet (*middle* planet from herein), with $1 M_{\oplus}$ and studied its orbital dynamics in the similar phase-spaces as displayed in Figs. 1 and 2.

Orbital parameters for an injected planet are chosen based on the stability zone observed for the inner planet. For each initial configuration, i_{pl} is varied from 0° - 90° , a_{pl} from 0.1 to 4 AU, and e_{pl} , Ω_{pl} and ω_{pl} are set close to zero while M is

randomly chosen between 0° - 360° . The mass is first set at $1 M_{\oplus}$, and later raised up to $20 M_{\oplus}$ to observe the orbital variations in the stability zone.

The *lifetime* map and the e_{max} map (Figs. 4 and 5) of the injected middle planet are also generated from its survival time in the orbits and the maximum eccentricity attained by the orbits during the total integrating period of 10 Myr, respectively. The maps indicate a wide stability region in the i_{pl} - a_{pl} phase-space. The blue region, lifetime, and the blue-green region (e_{max}) extend from 0.2 AU to 2.2 AU. The orbital inclination has a horizontal cutoff mark at $\sim 40^{\circ}$ which is due to the Kozai resonance, as seen in the e_{max} map. The eccentricity variation in this region of phase-space which is below 40° is less than 0.15 and all the orbits survive the total simulation time. Outside this stable zone, the planet’s eccentricity was forced to 0.4 or higher which caused it to either collide with the inner planet or get ejected from the system. In either case, the planet lost its orbital stability.

The gravitational influence of the inner planet around its orbits is small due to its small mass, while the outer planet’s gravitational influence reaches as far as 2 AU towards the star, generating number of orbital resonances. The observed resonances at the 1.40 AU, 1.70 AU, 1.93 AU, 2.00 AU, 2.25 AU and 2.70 AU are due to the 4:1, 3:1, 5:2, 7:3, 2:1 and 3:2 orbital resonances with the outer planet, respectively. Similar resonance structures are observed in the Solar System’s asteroid belt, where the *Kirkwood* gaps are in the 3:1, 5:2, 7:3, and 2:1 resonance with the Jupiter (Moons 1995).

To confirm that the dark blue-green regions as seen in Fig. 5, which we claim to be a stable zone for the middle planet, remains stable for more than 10 Myr, we picked few i_{pl} points along 1 AU mark (see Fig. 5, red asterisks) and integrated the whole system for 1 billion years. The time evolution of the planet’s eccentricity for three different orbital orientations are given in Fig. 6. The initial e_{pl} was set to zero and the planet was allowed to evolve in the gravitational influence of the three known bodies. For $i_{pl} = 0^{\circ}$ (Fig. 6, top panel), the amplitude of the eccentricity oscillations remains near the initial values for all three planets. The observed change in the eccentricity time series was less significant until the i_{pl} was set above 35° . For $i_{pl} = 40^{\circ}$ (Fig. 6, middle panel), the eccentricity for the inner and the middle planets start to display large

amplitude oscillations (0 to 0.4), but no violent end was observed during the billion year simulation time. Finally, for $i_{pl} = 45^\circ$ (Fig. 6, bottom panel) the middle planet’s eccentricity time-series varies significantly in its amplitude and eventually gets to 1. Then, the Earth-like planet collides with the inner planet when it is close to the billion year mark. 39.2° is the Kozai resonance mark, beyond which the anti-correlation between the e_{pl} and i_{pl} excites the orbits into high eccentricities, significantly reducing the periastron distance and leading to collisional path (for detailed Kozai resonance analysis, see Satyal (2014)). Therefore, we believe that the maximum inclination for the planets interior to the outer planet is less than the critical angle of 39.2° .

3.3. Analysis of Synthetic RV Signal

The orbits of the inner and the middle planets were simulated for 1500 days, with the high data sampling period (1 per day). The middle planet was first set at 1 AU with an assigned mass of $1 M_\oplus$, $5 M_\oplus$ and $10 M_\oplus$ in a near circular orbits and integrated separately for each mass. Then, using the integrated data, we generated a set of synthetic RV curves based on the RV signature of Keplerian motion given by equation 1, adapted from (Seager 2011). The synthesized RV curves for the inner planet (GJ 832c) and the middle planet with three different masses are plotted in Fig 7, top panel (a). The maximum amplitude of the RV signal for the inner planet is ~ 2.0 m/s, similar to the observational value reported by (Wittenmyer 2014). A bigger planet can produce a higher amplitude RV signal, however, the observation has constrained the RV signal for any new planets to be less than 2.0 m/s. For this reason we limited the planetary mass at $\leq 10 M_\oplus$, when placed at 1 AU because the higher mass planet would produce high amplitude RV.

$$V_r = \sqrt{G/(m_1 + m_2)a(1 - e^2)} \cdot m_2 \sin i \cdot [\cos(\omega + f) + e \cos \omega] \quad (1)$$

The injected planets at 1 AU display the RV curves with varying amplitude as expected. For the masses $1 M_\oplus$, $5 M_\oplus$ and $10 M_\oplus$, the RV signal is 0.14 m/s (black), 0.70 m/s (blue) and 1.04 m/s (green), respectively (Fig. 7, a). The RV amplitude for $1 M_\oplus$ is only ~ 0.14 m/s, which is much

smaller than the current high accuracy RV precision of about 0.97 m/s of the HARPS instruments. A planet interior to 1 AU could be less than $1 M_\oplus$ as well, however; it cannot be greater than $10 M_\oplus$ either. Bigger masses (for example $15 M_\oplus$) than these had RVs greater than 2 m/s, thus we disregarded the results. Any middle planet at 1 AU would have the orbital period of about ~ 550 days. Highlighted RV signal for $1 M_\oplus$ is shown in panel (b), with smaller y-axis variation.

The other two planets with masses $15 M_\oplus$ and $20 M_\oplus$ injected separately at 2 AU to obtain their synthetic RV reveal that $\sim 15 M_\oplus$ is the upper mass limit for the middle planet (Fig 7, bottom panel (c)) because its RV signal are measured less than 2.00 m/s. The RV signal for $15 M_\oplus$ (black) and $20 M_\oplus$ (blue) planets are 1.50 m/s and 2.10 m/s, respectively, and the orbital period is close to 1400 days. If the location is farther out towards the outer planet, the probable new planet has relatively higher mass than when it is closer towards the inner planet.

Now, based on the semi-amplitude values, $K = (V_{r,max} - V_{r,min})/2$, and a single measurement precision of σ we can estimate the minimum number of observations required to detect an exoplanet (adapted from Plavschan (2015)), and is given by:

$$N_{obs} = 2 \left(SNR \cdot \sigma / K \right)^2 \quad (2)$$

where the SNR is the detection confidence. The calculated N_{obs} based on the equation 2 for 5σ detection are given in Table 2. The N_{obs} for $1 M_\oplus$, $5 M_\oplus$ and $10 M_\oplus$ planets at 1 AU is 2500, 103 and 47, respectively; and for $15 M_\oplus$ at 2 AU, it is 23. The N_{obs} goes significantly higher for higher σ detection.

To check how the $i_{pl} - a_{pl}$ phase-space changes after injecting a planet with an upper mass limit, we re-simulated the system with $15 M_\oplus$ planet between the inner and outer planet (see Fig 8). The stability zone did not varied much compared to the $1 M_\oplus$ planet observed in Fig. 5. The inclination regime is reduced to 20° between 0.5 to 1.0 AU. The orbital resonances due to the outer planet continue to exist and limit the stability zone. From RV analysis we claimed that the $15 M_\oplus$ planet can reside at 2 AU from the star, and this phase-space map clearly indicates that the planet

has stable orbital configuration in this region for 10 Myr with small eccentricity variations.

The phase-space around the GJ 832c (black dashed line) has undergone least eccentricity variation compared to the e_{max} map in Fig. 5. This does not mean that the injected $15M_{\oplus}$ is stable in that region. The injected planet collides with the inner planet, which is smaller ($5.4M_{\oplus}$) than the injected planet, hence changing the orbital configuration of the inner planet and making it dynamically unstable. But the e_{max} for the $15M_{\oplus}$ planet remained close to its nominal value, and this is what we have plotted in the map.

4. Summary

The *lifetime* maps, e_{max} maps, and the time evolution of the orbital elements for GJ 832c indicates the stable orbital configuration for its best-fit orbital solutions. The maximum eccentricity deviation remained within the best-fit uncertainty values. Based on the e_{max} maps for the phase-spaces in i_{pl} , e_{pl} and a_{pl} , the relative inclination of the planet is less than 40° , maintains low eccentricity deviations and stable orbits for up to the integration period. The outer planet, GJ 832b extends its influence as far as 2.00 AU towards the star generating numerous resonances in the e_{pl} - a_{pl} phase-spaces. Due to this, the region starting from 2 AU to 3.56 AU remains dynamically unstable.

The i_{pl} regime of GJ 832c did not vary much even when an Earth-mass planet was injected into the system. The injected planet also maintained stable orbital configuration for the relative orbital inclination as high as 40° and the semimajor axis ranging from 0.2 to 2.2 AU. The maximum e_{pl} variation remained low suggesting a dynamically stable zone.

The injected middle planet could be smaller or bigger than the Earth-mass. However, its upper mass limit is limited by the radial velocity signal for the known inner planet (2m/s). Using this RV constraint, synthetic RV is generated from our simulation data. We obtained several RV curve for varying masses and distances for the middle planet. If the planet is located around 1 AU, it has upper mass limit of $10 M_{\oplus}$ and generated RV signal of 1.4 m/s. $1 M_{\oplus}$ planet at the same location has RV signal of 0.14 m/s only, much smaller

than the sensitivity of available technology. However, the RV detection is plausible for significantly large number of observations: ~ 2500 for $1 M_{\oplus}$ planet. The number of observation is reduced to 47 for $10 M_{\oplus}$ planet. The N_{obs} depends on the preferred σ detection value. Our aim here is just to provide a general idea to the observers.

When the middle planet was fixed to 2 AU, the upper mass limit increased to $15 M_{\oplus}$ with synthetic RV signal of 1.5 m/s. Hence, we expect a planet with mass less than $15 M_{\oplus}$ orbiting between the inner and the outer planets. Our RV signal calculations consider only 2 degree variation in i_{pl} . If the i_{pl} varies larger, the mass of the planet will vary according to *msini*. The orbital period of the planet at 1 AU and 2 AU are ~ 500 and ~ 1400 days, respectively.

The lower stability limit for an Earth-mass planet starts at 0.25 AU and the upper limit of the Star's classical habitable zone ends at 0.28 AU (from Kopparapu (2013)). Hence, there is a slim window of about 0.03 AU where an Earth-like planet could be stable as well as remain in the HZ.

Long-term orbital stability, orbital dynamics and the synthetic RV signal analysis suggests possible existence of an Earth-like planet between the inner and outer planets in the GJ 832 system. The anticipated RV signal is much lower than the sensitivity of the RV instruments; however, significantly large number of RV observations, the transit method, provided that the planets are along the line-of-sight, and the direct imaging are the viable options to get the observational verifications.

Acknowledgment We would like to thank The Office of Graduate Studies at UT Arlington and their I Engage Mentoring Program which initiated this research project to engage an undergraduate student (John Griffith). Also, many thanks to B. Quarles, M. Cuntz, J. Noyola for their comments and suggestions. Z.E.M. acknowledges the support of this reserach by the Alexander von Humboldt Foundation.

REFERENCES

- Bailey, J., Butler, R. P., Tinney, C. G., et al. 2009, ApJ, 690, 743
- Batalha, N. M., Rowe, J. F., Bryson, S. T., et al. 2013, ApJS, 204, 24

- Bonfils, X., Delfosse, X., Udry, S., et al. 2013, A&A, 549, A109
- Casagrande, L., Flynn, C., & Bessell, M. 2008, MNRAS, 389, 585
- Chambers, J. E. 1999, MNRAS, 304, 793
- Chambers, J. E., & Migliorini, F. 1997, in Bulletin of the American Astronomical Society, Vol. 29, AAS/Division for Planetary Sciences Meeting Abstracts 29, 1024
- Howard, A. W., Marcy, G. W., Bryson, S. T., et al. 2012, ApJS, 201, 15
- Jenkins, J. S., Jones, H. R. A., Tinney, C. G., et al. 2006, MNRAS, 372, 163
- Kopparapu, R. K. 2013, ApJ, 767, L8
- Mayor, M., Bonfils, X., Forveille, T., et al. 2009, A&A, 507, 487
- Quintana, E. V., Barclay, T., Raymond, S. N., et al. 2014, Science, 344, 277
- Seager, S. 2011, Exoplanets
- Wittenmyer, R. A., Tuomi, M., Butler, R. P., et al. 2014, ApJ, 791, 114
- Orosz, J. A., Welsh, W. F., Haghighipour, N., Quarles, B., Short, D. R., Mills, S. S., Satyal, S. et al. 2016, in Preparation
- Satyal, S., Hinse, T. C., Quarles, B., Noyola, J. P., 2014, MNRAS 443 1310
- Kozai, Y., AJ, 67,591
- Naoz, S., Farr, W. M., Lithwick, Y., Rasio, F. A., Teyssandier, J., 2013b, MNRAS, 431, 2155
- Ford, E. B., Kozinsky B., Rasio, F. A., 2000, ApJ, 535, 385
- Moons, M., Morbidelli, A., 1995, ICARUS 114, 33
- Plavchan, P., Latham, D., Gaudi, S., et al. 2015, arxiv 1503.01770

Table 1: Best-fit orbital parameters of the GJ 832 system obtained from Wittenmyer (2014). Mass of the star = $0.45 M_{\odot}$.

Parameters	GJ 832b	GJ 832c
Mass (M_{\oplus})	216 [188, 245]	5.4 [4.45, 6.35]
Semi-Major Axis (a)	3.56 AU [3.28, 3.84]	0.163 AU [0.157, 0.169]
Eccentricity (e)	0.08° [0.02, 0.1]	0.18° [0.05, 0.31]
Inclination (i)	$(0-90)^{\circ}$	$(0-90)^{\circ}$
Longitude of the Ascending Node (Ω)	0°	0°
Argument of the Periapsis (ω)	246° [224, 268]	10.0° [323, 57]
Mean Anomaly (μ)	307° [285, 330]	165° [112, 218]

Table 2: Radial Velocity semi-amplitude, $K = (V_{r,max} - V_{r,min})/2$, for varying mass and location, and estimated number of observations for different masses and up to 5σ detection.

Injected Planet Mass	Dist. from Star (AU)	RV semi-amplitude (m/s)	No. of Observations
$1 M_{\oplus}$	1	0.14	2500
$5 M_{\oplus}$	1	0.70	103
$10 M_{\oplus}$	1	1.40	47
$15 M_{\oplus}$	2	1.50	23

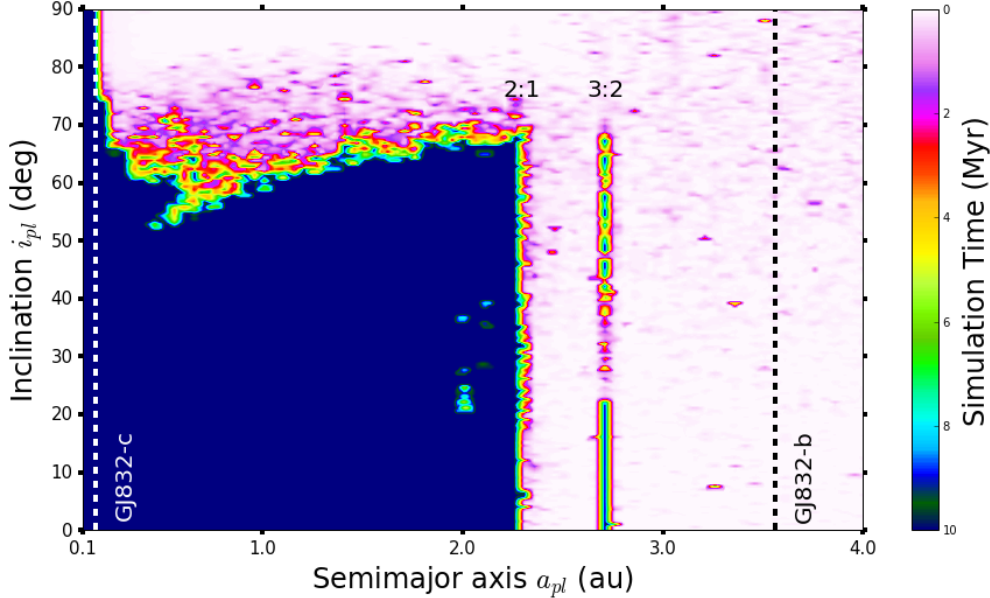


Fig. 1.— A global dynamical *lifetime* map of the inner planet, GJ 832c, in varying i_{pl} and a_{pl} phase-space, simulated for 10 Myr. The map represents the time evolution of the orbital elements with 14,000 initial conditions. The survival time (maximum 10 myr) is plotted in color coded z-axis. The color bar indicates the survival time, where the lighter colors represent the instability (ejection or collision) and the dark-blue color represents the stability (survival) up to the integration period. Hence, the dark blue-green region in the map is the dynamically stable zone. The vertical dashed lines at 0.16 AU and 3.56 AU represent the best-fit semi-major axis of inner and outer planets. The vertical islands at 2.25 and 2.7 AU are in 2:1 and 3:2 orbital resonance with the outer planet. These resonances are more prominent in phase-space map for e_{max} (Fig. 2).

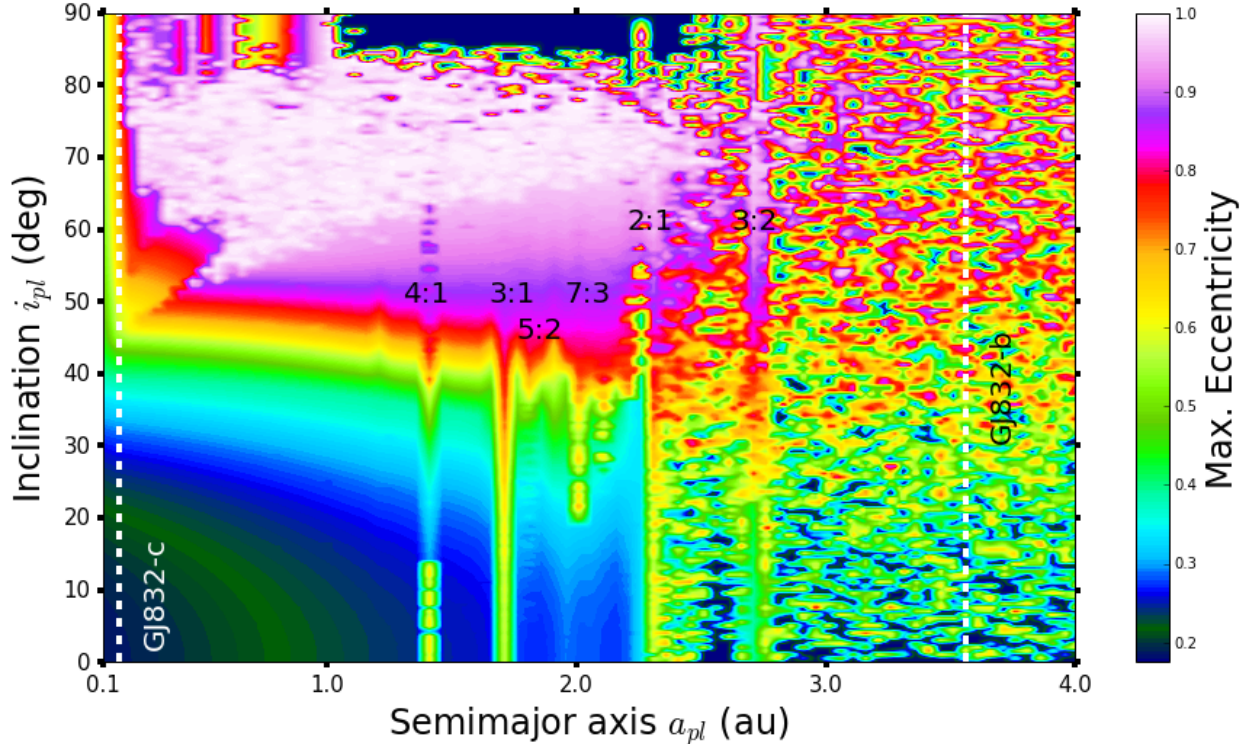


Fig. 2.— Maximum eccentricity, e_{max} map of the inner planet, GJ 832c, in i_{pl} and a_{pl} phase-space, simulated for 10 Myr. The map represents the time evolution of planet’s eccentricity for 14,400 initial conditions. The color bar indicates the e_{max} reached by the planet during the total simulation time, which also includes the cases when the planet suffers an ejection or collision (especially when e_{pl} reaches a value greater than 0.7). The dark blue-green color represents the best-fit e_{pl} value from the observational data (~ 0.18) and other light colors represent the deviation of e_{pl} from its nominal value to the observed e_{max} for the respective choices of initial conditions in i_{pl} and a_{pl} . The vertical white dashed lines denote the best-fit semi-major axis of the planets. The observed resonances at 1.4, 1.7, 1.9, 2.0, 2.25 and 2.7 AU are in 4:1, 3:1, 5:2, 7:3, 2:1, and 3:2 orbital resonance with the outer planet. Similar resonances (3:1, 5:2, 7:3 and 2:1) are observed in Solar System due to Jupiter’s influence in the Asteroid Belt, called Kirkwood gaps.

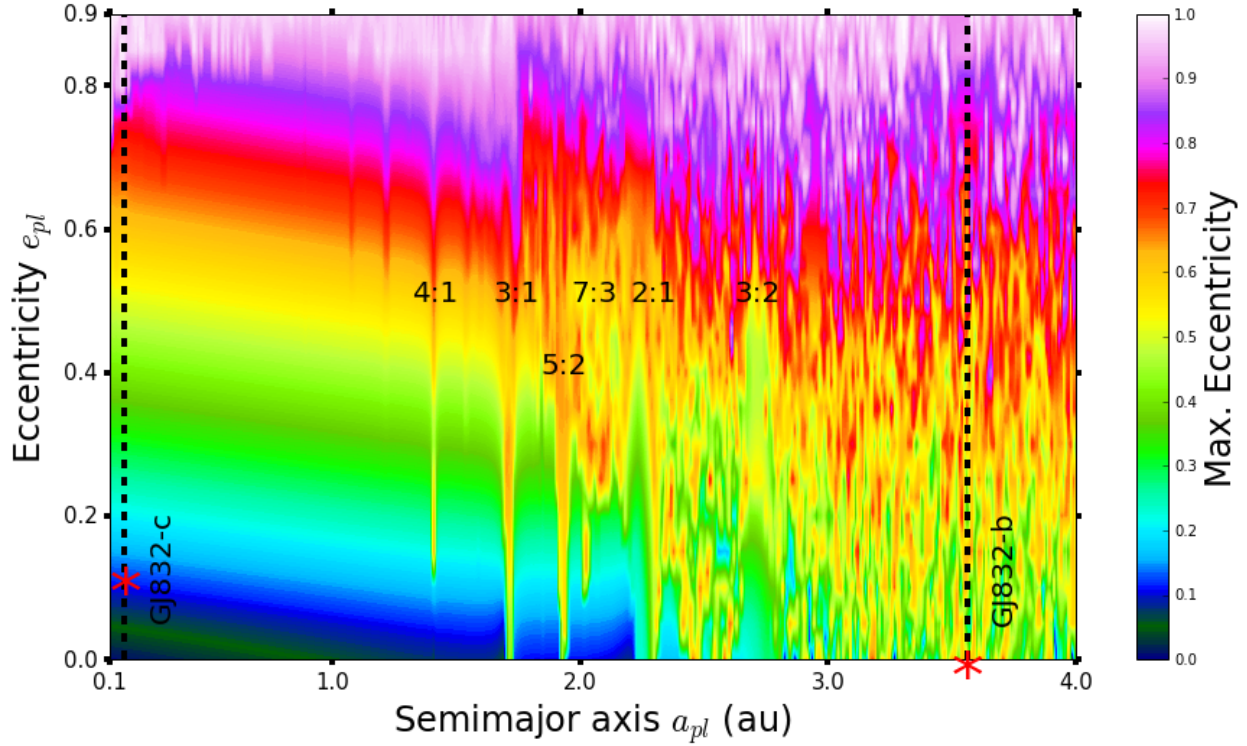


Fig. 3.— Maximum eccentricity, e_{max} map of the inner planet in $e_{pl} - a_{pl}$ phase-space, simulated for 10 Myr. The map represents the time evolution of planet’s eccentricity for different choices of initial conditions in e_{pl} and a_{pl} . The red asterisks denote the best-fit eccentricity value of the inner and middle planets, which shows no deviation from the nominal eccentricity values during the total integration period. The vertical resonance at 1.4, 1.7, 1.9, 2.0, 2.25 and 2.7 AU are in 4:1, 3:1, 5:2, 7:3, 2:1, and 3:2 orbital resonance with the outer planet.

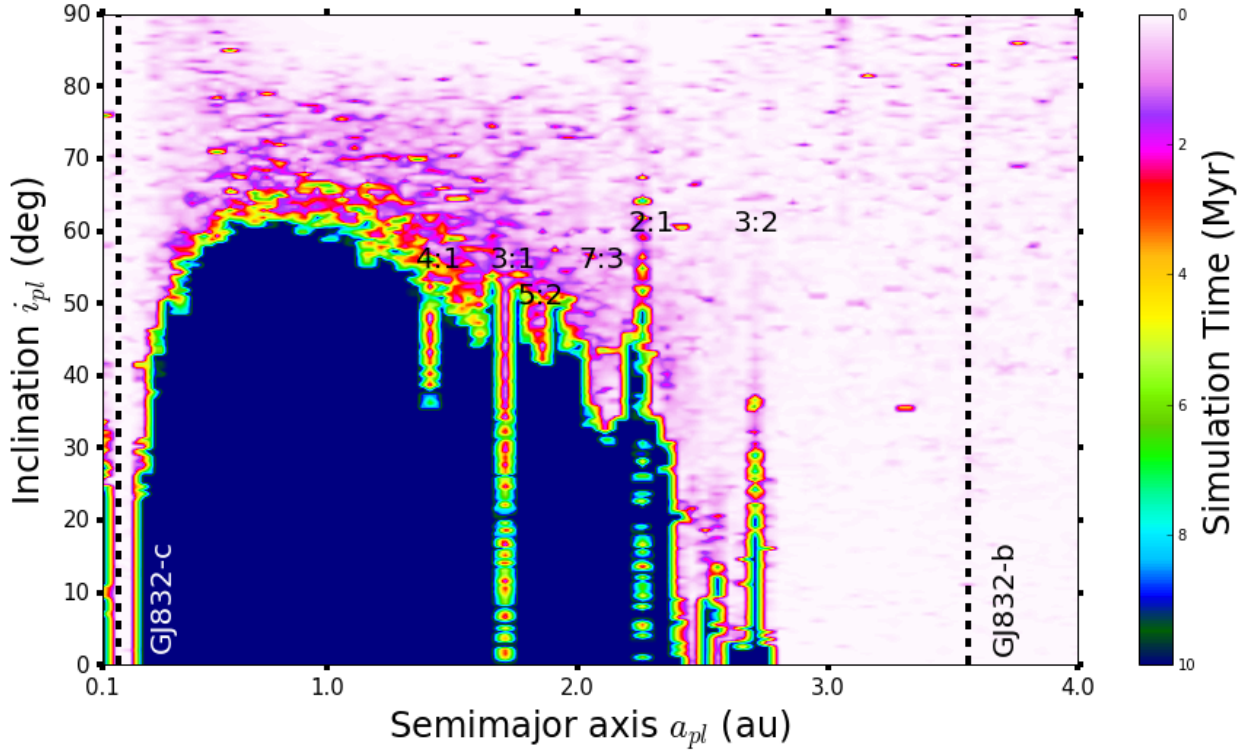


Fig. 4.— A global dynamical *lifetime* map of an Earth-mass middle planet in GJ 832 system injected in the dynamically stable zone (observed in Fig. 2) between the inner and the outer planet. The map represents the time evolution of orbital elements with 14,400 initial conditions for varying i_{pl} and a_{pl} and simulated for 10 Myr. The color bar indicates the survival time, where the lighter colors represent the instability (ejection or collision) and the dark-blue color represents the stability (survival) up to the integration period. The vertical dashed lines are the locations of the best-fit semi-major axis of the two known planets. The dark-blue region indicates the stable orbital configuration for the Earth-mass planet. the resonances due to the outer planet are similar to that observed in Fig. 2.

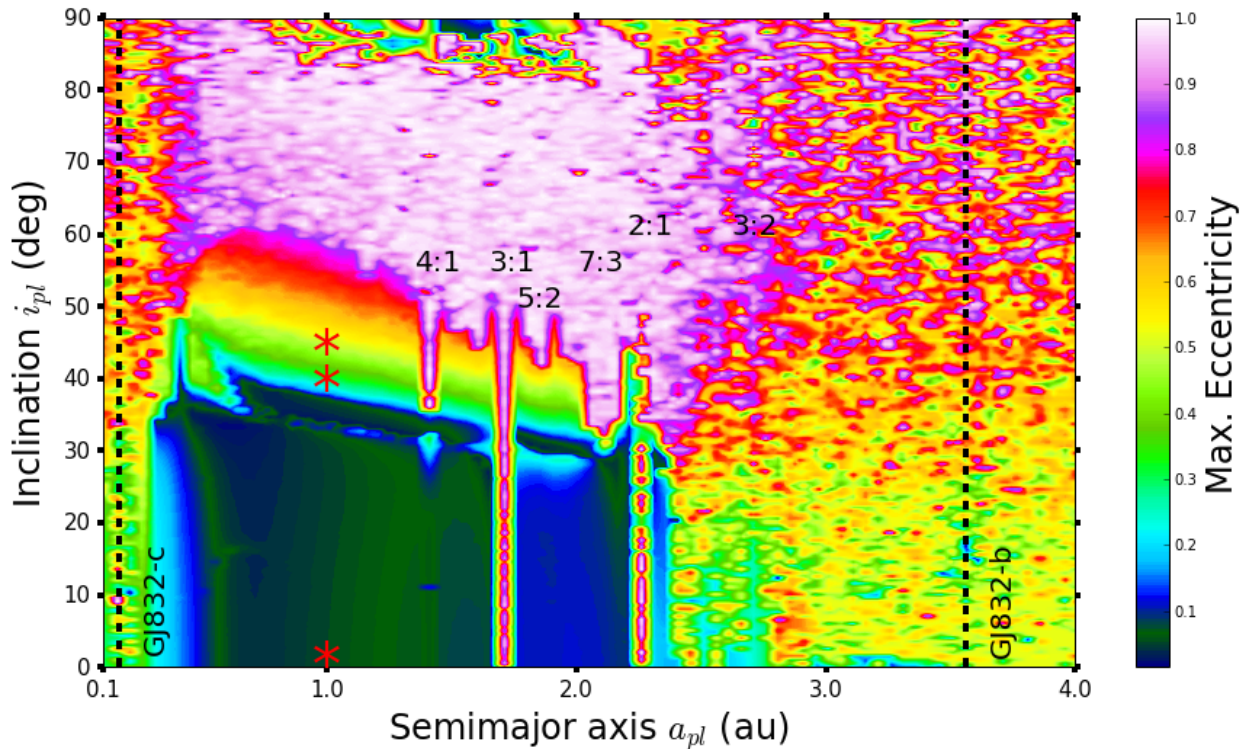


Fig. 5.— Maximum eccentricity (e_{max}) map of the Earth-mass planet injected between the inner and outer planets, in the i_{pl} and a_{pl} phase-space. The map represents the time evolution of planet’s eccentricity for 14,400 initial conditions, simulated for 10 Myr. The color bar indicates the e_{max} the orbit evolved into starting from 0.001 during the total simulation time. The e_{pl} varies less from 0.2 to 2.2 AU and below 40° . In any other cases, the planet suffered an ejection or collision with the inner or outer planets, especially when e_{pl} reaches a value greater than 0.5. The dark blue-green color represents the best-fit e_{pl} parameter from observation (0.18) and other light color represent the e_{max} value the planet attained for the respective choices of initial conditions in i_{pl} and a_{pl} . The vertical dashed line are the best-fit semi-major axis of the two known planets, and the resonances due to the outer planet are similar to that observed in Fig. 2. The three specific locations, denoted by the red asterisks, are explored for a billion years orbital evolution in Fig. 6 in an attempt to constrain the injected planet’s i_{pl} and e_{pl} and observe the orbital evolution in time series.

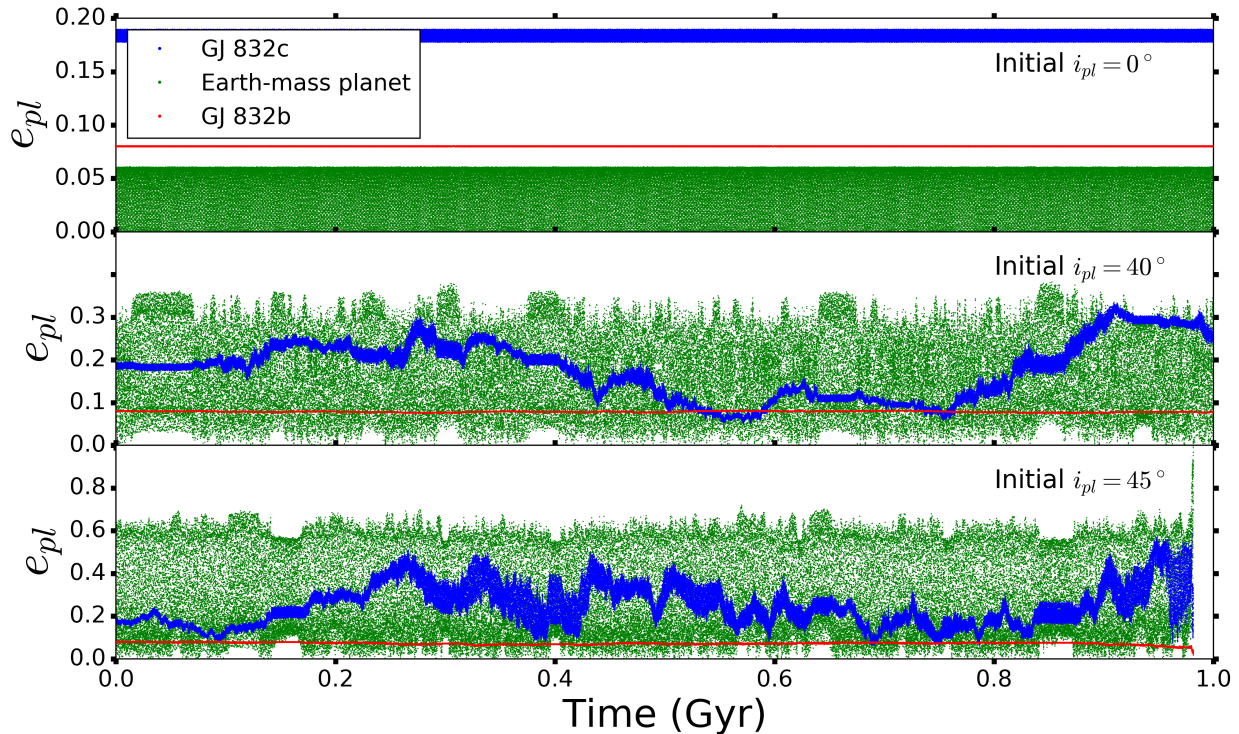


Fig. 6.— Time evolution of eccentricity for the middle planet ($1 M_{\oplus}$) set at 0° (top), 40° (middle), and 45° (bottom) relative inclination and semimajor axis along 1 AU. The nominal values of e_{pl} were used for the inner and outer planets, and the initial e_{pl} for the middle planet was set at 0.001. For $i_{pl} = 0^\circ$, the eccentricity evolution is smooth with minimal deviation from its initial value for all three planets. The amplitude of e_{pl} oscillations slowly increases as the i_{pl} is raised higher, and is highly noticeable for the middle and inner planets when $i_{pl} = 40^\circ$. The e_{pl} fluctuations is between 0.0 and 0.4 and it goes to 1 when the i_{pl} is set at 45° , hence arising the unstable orbital configuration. The injected planet does not influence the orbital evolution of the outer planet, and its eccentricity remains constant through out the simulation time.

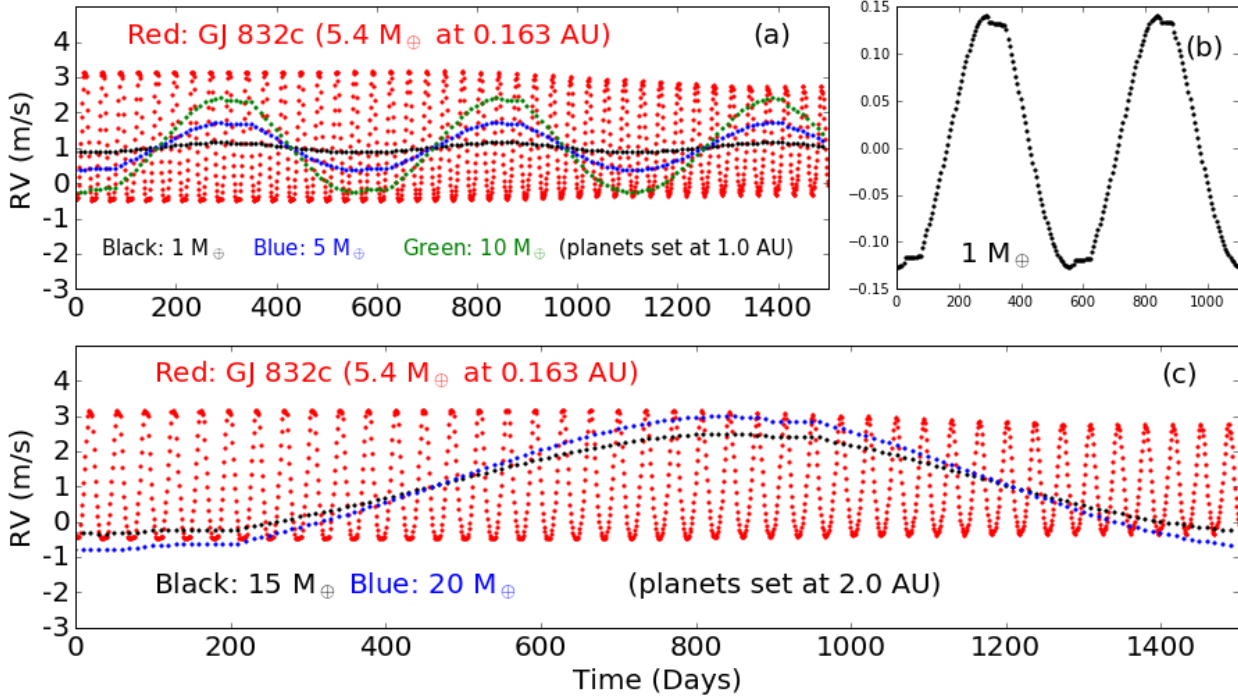


Fig. 7.— (a): Synthetic radial velocity signature of Keplerian motion is shown for the inner planet GJ 832c (red) and the middle planet at 1 AU for 3 different masses. The black, blue and green curves represents the RV signal for $1 M_{\oplus}$, $5 M_{\oplus}$ and $10 M_{\oplus}$, respectively. The maximum amplitude (2.0 m/s) is for the inner planet which is much closer to the star than the injected planet at 1 AU whose amplitude varies by mass: 0.14 m/s, 0.7 m/s and 1.04 m/s for masses $1 M_{\oplus}$, $5 M_{\oplus}$ and $10 M_{\oplus}$, respectively. The RV indicates that the orbital period for these planets to be about ~ 550 days. (b): Synthetic RV signal plotted for $1 M_{\oplus}$ with smaller y-axis variation. (c): Synthetic RV signal for the planets injected at 2 AU having masses $15 M_{\oplus}$ and $20 M_{\oplus}$ with an amplitude 1.50 m/s and 2.1 m/s. The RV signal for the $20 M_{\oplus}$ planet exceeds the RV signal from the detected inner planet. So the upper limit for the planet’s mass, if it is at 2 AU, is $\sim 15 M_{\oplus}$ and the orbital period of ~ 1400 days.

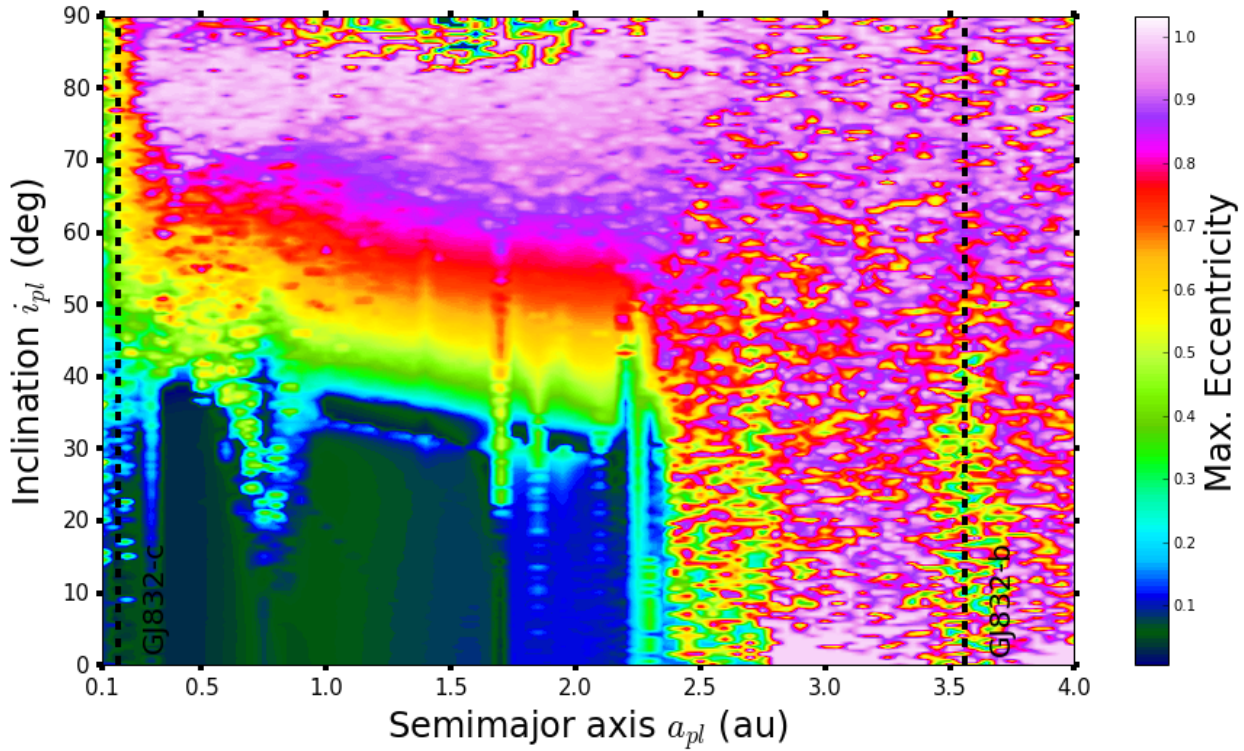


Fig. 8.— Maximum eccentricity (e_{max}) map of the 15 Earth-mass planet between inner and outer planets, in the i_{pl} and a_{pl} phase-space, simulated for 10 Myr. This map is similar to the one for $1 M_{\oplus}$ shown in Fig. 5, but for higher mass. The stability regime in the phase-space is reduced from 40° to 20° between 0.5 AU to 1 AU, but based on our RV signal analysis, more likely location for this planet is around 2 AU. The e_{pl} around 2 AU regions have evolved to 0.2 from 0.001, in 10 Myr. Thus, any such planet will have eccentric orbit, nonetheless, it maintains stable orbital configuration.